Macromolecules

Volume 40, Number 23 November 13, 2007

Communications to the Editor

Anisotropic Ion Conductivity in Liquid Crystalline Diblock Copolymer Membranes with Perpendicularly Oriented PEO Cylindrical Domains

Jingze Li,[†] Kaori Kamata,[†,§] Motonori Komura,[†] Takeshi Yamada,[‡] Hirohisa Yoshida,[‡,§] and Tomokazu Iyoda*[,†,§]

Division of Integrated Molecular Engineering, Chemical Resources Laboratory, Tokyo Institute of Technology, R1-25, 4259 Nagatsuta-cho, Midori-ku, Yokohama 226-8503, Japan, and Department of Applied Chemistry, Faculty of Urban Environmental Sciences, Tokyo Metropolitan University, 1-1 Minami-Osawa, Hachiouji, Tokyo 192-0397, Japan, and CREST, Japan Science and Technology Agency, 4-1-8 Hon-cho, Kawaguchi, Saitama 332-0012, Japan

Received August 13, 2007
Revised Manuscript Received September 25, 2007

Nanostructured polymer membranes that exhibit anisotropic ion transport have attracted much attention recently because they can be exploited as scaffolds and templates for efficient fabrication of various nanoscopic structures/objects,[1,2] as well as in electrochemical systems, such as high performance lithium ion batteries[3−6] and fuel cells.[7−9] In principle, a physical approach was used for preparing anisotropic polymer membranes containing low-dimensional ion conductors. For example, one-dimensional (1D) conductivity has been demonstrated in a track-etched polycarbonate membrane with nanopores, which were infiltrated with lithium ion or proton conductive polymers.[10,11] From the viewpoints of practical application and mass production, a chemical approach based on self-organization seems to offer the promising potential for introduction of anisotropic nanostructures to ion conducting materials, as the following remarkable progress has been made so far.[3−8] A variety of materials, including ionic liquids,[12] liquid crystalline (LC) materials,[5,13−16] block copolymers,[9,17−20] dendrimers,[21] and supramolecules,[22] have been synthesized for the purpose of preparing nanostructured ion conductors with geometries varying from columnar[12,22] and layered[13−15,23] to gyroidal structures.[8,21] When using the chemical methods to prepare patterned membranes, it is essential to have uniform alignment and coaxial orientation of the phase-segregated nanostructures on the macroscopic scale to guarantee a large and reproducible anisotropy. In light of their potential application to electrochemistry, the conductive nanochannels should be aligned perpendicular to the electrode surface.[3,24] Especially, Kato and Ohno succeeded in demonstrating both high conductivity and its large anisotropy up to three orders of magnitude in well-designed LC ionic liquid materials.[3] Their success includes a smart surface modification of the electrodes on the conductivity measurement with an organic monolayer so as to control the surface energy[25] and as a result, to align ion-conductive channels normal to the electrode surface.[3,16] In principle, the conductivity anisotropy includes both how efficiently the ions can be migrated along the designed ion channels and how effectively the transport in the orthogonal directions can be blocked by the designed anisotropic nanostructure. Although the average anisotropic nanostructures have been analyzed so far by small-angle X-ray scattering (SAXS) or polarized optical microscopes, microscopic observation such as TEM and AFM will be preferable to evaluate the local disorder or defects.

Here, we report an anisotropic lithium ion conductivity in phase-segregated LC diblock copolymer membranes with perpendicularly oriented poly(ethylene oxide) (PEO) cylindrical domains as ion transport channels, which can be well visualized by recently developed cross-sectional AFM imaging.[26] De Jeu and co-workers have already demonstrated effective orientation of upright lamella[27] or cylinder[28] nanostructures in thin films by introducing LC side chain in hydrophobic polystyrene-*b*-polymethacrylate derivatives.[29] The present diblock copolymer thick membrane was endowed with amphiphilicity as a stronger chemical contrast by choosing hydrophilic PEO,[30] leading to

* To whom correspondence should be addressed. Telephone: 81-45-924-5266. Fax: 81-45-924-5247, E-mail: iyoda.t.aa@m.titech.ac.jp.
[†] Tokyo Institute of Technology.
[‡] Tokyo Metropolitan University.
[§] Japan Science and Technology Agency.

10.1021/ma071821s CCC: $37.00
Published on Web 10/13/2007

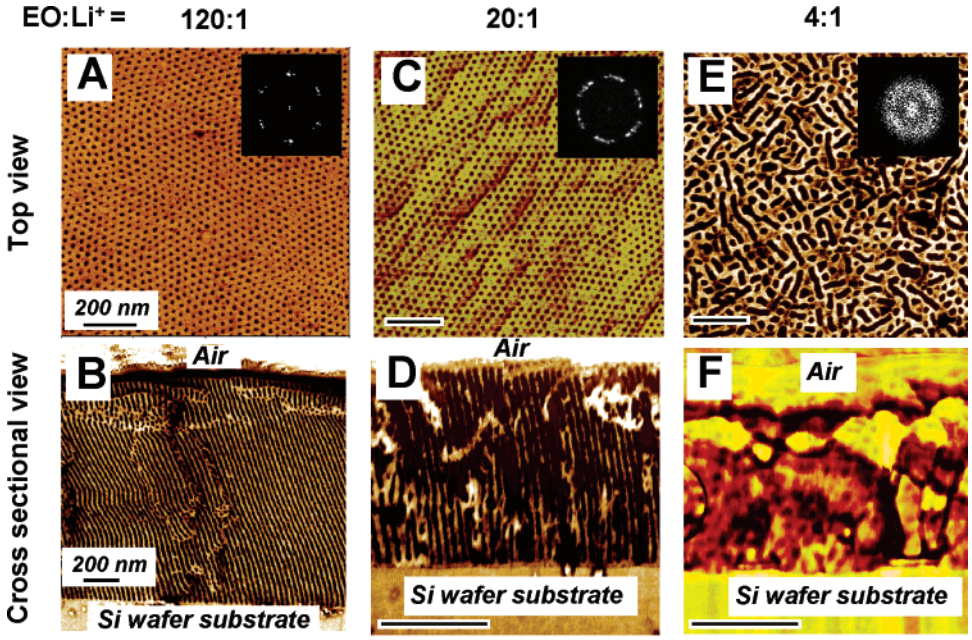

Figure 1. AFM phase images of PEO_{114}-*b*-$PMA(Az)_{47}$ + $LiCF_3SO_3$ membranes at different EO:Li^+ ratios. Key: (A, B) 120:1; (C, D) 20:1; (E, F) 4:1. The top images are surface morphologies of the membranes, and the bottom images are their cross sections. Insets are the corresponding fast Fourier transformation images.

domain-selective hybridization with additives and specific reaction field to the space-restricted domains.[2,24] As a result, a unique ordered nanostructure, wherein an array of hexagonally arranged and perpendicularly oriented PEO nanocylinders span both surfaces, beyond microscopic view to a meter-length scale, can be fabricated just by using simple thermal annealing without any special surface treatment.[24,26]

Selective doping of lithium salt into the PEO cylindrical domains was achieved during the microphase segregation, i.e., just by mixing an appropriate amount of $LiCF_3SO_3$ with 4 wt % of toluene solution containing the copolymer, coating onto the desired substrate, and annealing at 140 °C for 24 h. The microphase segregation forces the PEO cylindrical domains containing the lithium salt to be hexagonally arranged and normally oriented in the hydrophobic PMA(Az) domain matrix. The LC ordering as smectic phase ensures the macroscopically unidirectional orientation[27,28] of the PEO cylindrical domains.[30−35] The doped salt concentration has an influence on the nanostructure of the membrane including periodicity and orientation of the ion conducting PEO nanochannel array. Figure 1 shows the structural evolution of the polymeric electrolyte membrane as a function of the salt concentration as probed by atomic force microscopy (AFM) in the phase mode. When a small amount of salt was doped into the copolymer, i.e., EO:Li^+ = 120:1 for the PEO_{114}-*b*-$PMA(Az)_{47}$ + $LiCF_3SO_3$ complex (The amount of the doped salt is described by the molar ratio of an ethylene oxide (EO) unit in the PEO to the cation), a hexagonally arranged PEO dot array was observed as a (001) face of the hexagonally arranged cylinder phase.[26] Furthermore, the periodic nanocylinder array preferentially oriented perpendicular to the substrate surface, which was assisted by LC cooperative motion of the azobenzene mesogen.[26,30−35] Most of the cylinders with a diameter of around 11 nm can span the entire membrane, i.e., from one interface to the other. The nanostructure of the complex is similar to that of a pure copolymer film.[30−35] These structural features were preserved at an EO:Li^+ ratio of 20:1, that is, well-ordered nanocylinders were predominantly formed vertical to the substrate surface, which exhibited a slightly enlarged periodicity with increasing salt concentration. A serious

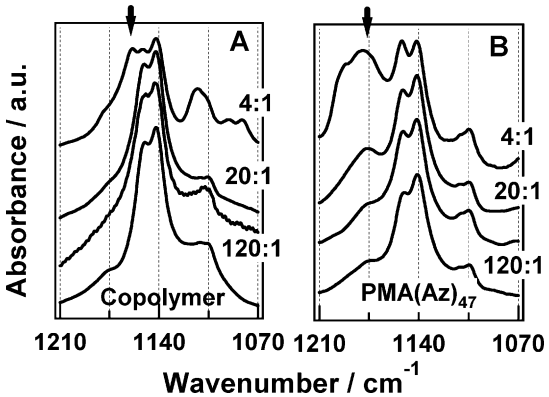

Figure 2. FTIR spectra of complexes of PEO_{114}-*b*-$PMA(Az)_{47}$ + $LiCF_3SO_3$ (A) and $PMA(Az)_{47}$ + $LiCF_3SO_3$ (B) over a range of EO:Li^+ ratios. The arrow in part A indicates a 1160 cm^{-1} peak, and the arrow in part B indicates a 1180 cm^{-1} peak, which represent asymmetric stretching modes of CF_3 of the counteranion of the salt.

change in membrane morphology was observed as the salt amount approached 4:1, where many in-plane-laid cylindrical domains appear with the normally oriented ones on the surface. The diameters of both rods and dots observed become larger due to a heavy amount of the doped salt. More clearly, a serious disorder was found in the cross-sectional image (Figure 1F). Both regularity of the PEO cylindrical domains and their orientation become considerably worse. The structural evolution described above was confirmed independently by SAXS measurements of the pellet samples (see Supporting Information). Although the hexagonal structural pattern is still preserved even in the case of larger amount of the salt, both the regularity and orientation of the PEO nanocylinder array is seriously disordered.

To determine whether the salt was selectively hosted by the PEO domains of the block copolymer, Fourier-transform infrared (FTIR) spectral analysis was performed as a function of salt concentration (Figure 2A). As a reference, the FTIR spectra of homopolymer-based complexes of $PMA(Az)_{47}$ + $LiCF_3SO_3$ are presented in Figure 2B. The spectrum of the pure copolymer

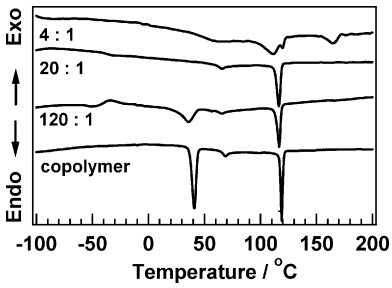

Figure 3. DSC thermographs of PEO_{114}-*b*-$PMA(Az)_{47}$ and its complexes doped by $LiCF_3SO_3$ at different ratios of EO:Li^+ = 120:1, 20:1, and 4:1, obtained upon the second heating procedure at a scanning rate 10 °C/min.

exhibits two strong absorption bands at 1151 and 1142 cm^{-1}, which are ascribed to stretching vibrations of C−O−C bonds in PEO main chain and PMA(Az) side chain.[36] As the amount of the added salt increased, the FTIR spectra of the homopolymer and copolymer changed in different manners. For the homopolymer, $PMA(Az)_{47}$ + $LiCF_3SO_3$, the intensity of the peak centered at 1180 cm^{-1} increases noticeably with increasing salt concentration, whereas little increase was observed for the copolymer. In contrast, a new peak appears at 1160 cm^{-1} for the copolymer at EO:Li^+ = 4:1, as well as in PEO homopolymer (see Supporting Information).[36] Both 1180 and 1160 cm^{-1} peaks are assigned to asymmetric stretching modes of CF_3 in the counteranion of the salt, which have been used as probe sensitive to its local environment.[36] The different performances of asymmetric stretching modes of CF_3 in copolymer, PMA(Az) homopolymer and PEO homopolymer systems indicate that lithium salt is mainly dissolved within the PEO domain, leading to the formation of ion-transporting nanochannels surrounded by ion-insulating PMA(Az) segments. At high concentrations, salt may be distributed within the PMA(Az) matrix of the block copolymer, as indicated by a slight change in the shoulder peak at 1180 cm^{-1}.

Differential scan calorimetry (DSC) measurements further clarify the structural evolution. Figure 3 depicts DSC traces of complexes at various salt concentrations. In the case of the pure copolymer, there are two well-defined endothermic transitions at 37 and 117 °C and a small transition at around 65 °C. These transitions represent melting of the crystalline PEO domain, transition from the smectic A to the isotropic phase, and that from the smectic X to the smectic C phase, respectively.[30,32] At low salt concentrations (EO:Li^+ = 120:1), there was a rapid reduction in the enthalpy indicated by the PEO melting peak. On the basis of the enthalpy value, the PEO crystallinity is estimated to be about 46% of that of the pure copolymer. This reduction in crystallinity is desirable for ion transport because it is generally accepted that ionic conductivity occurs primarily through amorphous regions.[5,17] At medium concentrations (EO:Li^+ = 20:1), the melting peak entirely disappeared, indicating the PEO domain is fully amorphous. In contrast to this copolymer system, variation in the salt concentration has a very limited impact on reducing the crystallinity in PEO homopolymer system.[36] The difference is likely to be related to size confinement effect of the nanocylinders.[37] On the other hand, there was no significant change in the transition from the smectic A to the isotropic phase for samples prepared at EO:Li^+ ratios of 120:1 and 20:1. However, at high salt concentration (EO:Li^+ = 4:1), there was a dramatic broadening in the isotropic transition temperature range. This change suggests the alignment of the LC domain was greatly disturbed, which was consistent with the disordered structure observed by AFM. In addition, an endothermic peak was observed at 147 °C at this concentration, representing the melting of a newly formed stoichiometric coordination crystalline.[36]

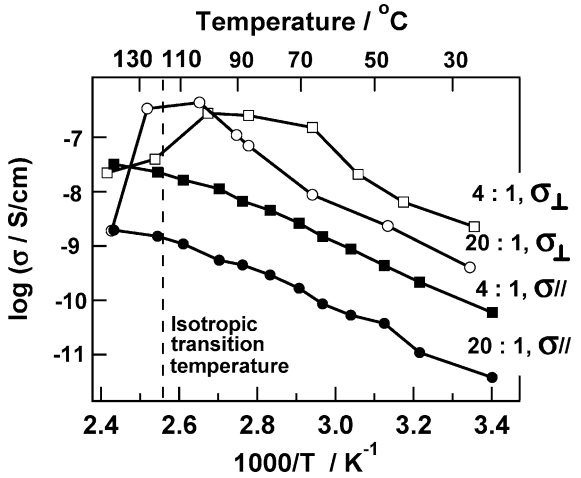

Figure 4. Anisotropic ion conductivity of PEO_{114}-*b*-$PMA(Az)_{47}$ + $LiCF_3SO_3$ complexes as a function of temperature for EO:Li^+ ratio at 20:1 and 4:1; perpendicular (○, □) and parallel (●, ■) to the substrate.

Figure 4 shows the temperature dependence of the ion conductivities perpendicular ($\sigma_\perp$) and parallel ($\sigma_\parallel$) to the substrate at two salt concentrations. At an EO:Li^+ ratio of 20:1, the $\sigma_\perp$ conductivity initially increases with the increasing temperature. Above the transition temperature from the smectic A to the isotropic phase, the $\sigma_\perp$ conductivity abruptly drops. The same tendency was observed at the higher salt concentration (EO:Li^+ = 4:1), although an increase in $\sigma_\perp$ conductivity was not so high as expected one. On the contrary, the $\sigma_\parallel$ conductivity behaves in a different manner, exhibiting a monotonous increase with increasing temperature for EO:Li^+ ratios of 20:1 and 4:1. Moreover, the $\sigma_\perp$ conductivity is always larger than the $\sigma_\parallel$ conductivity in the smectic phase. The maximum anisotropies ($\sigma_\perp/\sigma_\parallel$) reach 450 and 40 for EO:Li^+ ratios of 20:1 and 4:1, respectively.

It is apparent that when the salt concentration is not too high, i.e., at EO:Li^+ ratios from 120:1 to 20:1, the complex can inherit the unique structural properties of the diblock copolymer very well (see Supporting Information). The $LiCF_3SO_3$ is predominantly dissolved in the PEO domains, which play an important role as 1D ion transport channels with decananometer diameter across the entire membrane. In addition, a loose cross-linking effect of the Li^+-coordinated PEO chains can effectively suppress PEO crystallization in the limited nanospace. These factors would lead to highly anisotropic conductivity. However, at even higher concentration (EO:Li^+ = 4:1), a number of Li^+ could bring about a kind of strong cross-linking effect in the PEO domains due to the formed stoichiometric coordination crystalline,[36] and furthermore, some of them might interact with the ester and/or ether groups even in the hydrophobic PMA(Az) domains. These effects would disrupt both LC ordering and the inherent microphase separation.[38] It should be noted that the moderate anisotropy obtained here, 450 at EO:Li^+ = 20:1, as well as relatively low conductivity, might be due to the strict measurement of $\sigma_\perp$ conductivity of the membrane with its thickness larger than 50 μm so as to avoid any electrical leakage. Our ongoing work is to develop the conductivity measurement by using a thinner reliable film with much less defects and simultaneously evaluating the quality of the nanostructures, which is just our motivation in this field.

In summary, we demonstrated the anisotropic ion transport behavior in phase-segregated electrolytic membranes by selective doping of $LiCF_3SO_3$ into the PEO domains of LC

amphiphilic diblock copolymers. The perpendicularly aligned PEO cylindrical array containing Li^+, visualized directly by AFM cross-sectional mapping, provides straight ion transport paths as 1D nanoconductors, resulting in effective conductivity achieved vertical to the substrate surface. The findings will promote the development of novel polymer materials with faster ion transport and larger anisotropic conductivity than existing materials.

Acknowledgment. This work was partly supported by a Grant-in-Aid for Scientific Research (No. 15201024) from the ministry of Education, Culture, Sports, Science, and Technology, Japan. J.L. expresses thanks for a postdoctoral fellowship from Japanese Society for the Promotion of Science.

Supporting Information Available: Text giving experimental details and figures showing representative chemical structure, membrane structure, SAXS profiles, FTIR spectra, and configurations of conductivity measurements. This material is available free of charge via the Internet at http://pubs.acs.org.

References and Notes

(1) Lazzari, M.; Lopez-Quintela, M. A. *Adv. Mater.* **2003**, *15*, 1583−1594.
(2) Li, J. Z.; Kamata, K.; Watanabe, S.; Iyoda, T. *Adv. Mater.* **2007**, *19*, 1267−1271.
(3) Kato, T.; Mizoshita, N.; Kishimoto, K. *Angew. Chem., Int. Ed.* **2006**, *45*, 38−68.
(4) Kato, T. *Science* **2002**, *295*, 2414−2418.
(5) Zheng, Y. G.; Lui, J. G.; Ungar, G.; Wright, P. V. *Chem. Rec.* **2004**, *4*, 176−191.
(6) Livshits, E.; Kovarsky, R.; Lavie, N.; Hayashi, Y.; Golodnitsky, D.; Peled, E. *Electrochim. Acta* **2005**, *50*, 3805−3814.
(7) Ikkala, O.; ten Brinke, G. *Science* **2002**, *295*, 2407−2409.
(8) Ikkala, O.; ten Brinke, G. *Chem. Commun.* **2004**, 2131−2137.
(9) Cho, G. J.; Park, K. P.; Jang, J. K.; Jung, S. G.; Moon, J.; Kim, T. *Electrochem. Commun.* **2002**, *4*, 336−339.
(10) Vorrey, S.; Teeters, D. *Electrochim. Acta* **2003**, *48*, 2137−2141.
(11) Chen, H.; Palmese, G. R.; Elabd, Y. A. *Chem. Mater.* **2006**, *18*, 4875−4881.
(12) Yoshio, M.; Mukai, T.; Ohno, H.; Kato, T. *J. Am. Chem. Soc.* **2004**, *126*, 994−995.
(13) Ohtake, T.; Ogasawara, M.; Ito-Akita, K.; Nishina, N.; Ujiie, S.; Ohno, H.; Kato, T. *Chem. Mater.* **2000**, *12*, 782−789.
(14) Yoshio, M.; Mukai, T.; Kanie, K.; Yoshizawa, M.; Ohno, H.; Kato, T. *Adv. Mater.* **2002**, *14*, 351−354.
(15) Kishimoto, K.; Yoshio, M.; Mukai, T.; Yoshizawa, M.; Ohno, H.; Kato, T. *J. Am. Chem. Soc.* **2003**, *125*, 3196−3197.
(16) Yoshio, M.; Kagata, T.; Hoshino, K.; Mukai, T.; Ohno, H.; Kato, T. *J. Am. Chem. Soc.* **2006**, *128*, 5570−5577.
(17) Judeinstein, P.; Roussel, F. *Adv. Mater.* **2005**, *17*, 723−727.
(18) Ruotsalainen, T.; Torkkeli, M.; Serimaa, R.; Makela, T.; Maki-Ontto, R.; Ruokolainen, J.; ten Brinke, G.; Ikkala, O. *Macromolecules* **2003**, *36*, 9437−9442.
(19) Sadoway, D. R. *J. Power Sources* **2004**, *129*, 1−3.
(20) Trapa, P. E.; Reyes, A. B.; Das Gupta, R. S.; Mayes, A. M.; Sadoway, D. R. *J. Electrochem. Soc.* **2006**, *153*, A1098−A1101.
(21) Cho, B. K.; Jain, A.; Gruner, S. M.; Wiesner, U. *Science* **2004**, *305*, 1598−1601.
(22) Percec, V.; Heck, J. A.; Tomazos, D.; Ungar, G. *J. Chem. Soc., Perkin Trans. 2* **1993**, 2381−2388.
(23) Kishimoto, K.; Suzawa, T.; Yokota, T.; Mukai, T.; Ohno, H.; Kato, T. *J. Am. Chem. Soc.* **2005**, *127*, 15618−15623.
(24) Kamata, K.; Iyoda, T. Nanocylinder array structures in block copolymer thin films. In *Nanomaterials from research to application*, Hosono, H., Mishima, Y., Takezoe, H., Mackenzie, K. J. D., Eds.; Elsevier Ltd.: London, 2006; pp 171−223.
(25) Mansky, P.; Liu, Y.; Huang, E.; Russell, T. P.; Hawker, C. *Science* **1997**, *275*, 1458−1460.
(26) Komura, M.; Iyoda, T. *Macromolecules* **2007**, *40*, 4106−4108.
(27) Wong, G. C. L.; Commandeur, J.; Fischer, H.; de Jeu, W. H. *Phys. Rev. Lett.* **1996**, *77*, 5221−5224.
(28) Al-Hussein, M.; Serero, Y.; Konovalov, O.; Mourran, A.; Moller, M.; de Jeu, W. H. *Macromolecules* **2005**, *38*, 9610−9616.
(29) Li, L. B.; de Jeu, W. H. *Phys. Rev. Lett.* **2004**, *92*, 75506−3.
(30) Tian, Y. Q.; Watanabe, K.; Kong, X. X.; Abe, J.; Iyoda, T. *Macromolecules* **2002**, *35*, 3739−3747.
(31) Yu, H. F.; Okano, K.; Shishido, A.; Ikeda, T.; Kamata, K.; Komura, M.; Iyoda, T. *Adv. Mater.* **2005**, *17*, 2184−2188.
(32) Jung, S. Y.; Yamada, T.; Yoshida, H.; Iyoda, T. *J. Therm. Anal. Calorim.* **2005**, *81*, 563−567.
(33) Yu, H. F.; Li, J. Z.; Ikeda, T.; Iyoda, T. *Adv. Mater.* **2006**, *18*, 2213−2215.
(34) Yu, H. F.; Iyoda, T.; Ikeda, T. *J. Am. Chem. Soc.* **2006**, *128*, 11010−11011.
(35) Watanabe, S.; Fujiwara, R.; Hada, M.; Okazaki, Y.; Iyoda, T. *Angew. Chem., Int. Ed.* **2007**, *46*, 1120−1123.
(36) Dissanayake, M.; Frech, R. *Macromolecules* **1995**, *28*, 5312−5319.
(37) Muller, A. J.; Balsamo, V.; Arnal, M. L.; Jakob, T.; Schmalz, H.; Abetz, V. *Macromolecules* **2002**, *35*, 3048−3058.
(38) Epps, T. H.; Bailey, T. S.; Waletzko, R.; Bates, F. S. *Macromolecules* **2003**, *36*, 2873−2881.

MA071821S